

Distortions of Gallium Octahedra in Ba_5Ga_6 and the Likelihood of the Reported Phase Being $\text{Ba}_5\text{Ga}_6\text{H}_2^\dagger$

Qiang Liu and Roald Hoffmann*

Department of Chemistry and Materials Science Center, Cornell University, Ithaca, New York 14853–1301

John D. Corbett

Department of Chemistry and Ames Laboratory–DOE, Iowa State University, Ames, Iowa 50011

Received: May 10, 1994*

In the intriguing Ba_5Ga_6 phase of Fornasini and Pani, one finds isolated, nearly perfect octahedral Ga_6 clusters with one more skeletal electron pair (i.e., Ga_6^{10-}) than predicted by the Wade–Mingos rules. The electronic structures of the molecular Ga octahedron and Ba_5Ga_6 were studied by the extended Hückel method. According to our calculations, the octahedral cluster, either as isolated Ga_6^{10-} or in the extended Ba_5Ga_6 structure, appears to be unstable with respect to Jahn–Teller distortion. There is room for hydrides in the Ba_5Ga_6 structure; $\text{Ba}_5\text{Ga}_6\text{H}_2$ is an attractive formulation, for it should have, as our computations indicate, relatively undistorted Ga_6 octahedra in it.

Ba_5Ga_6 , an intermetallic binary compound, was reported recently by Fornasini and Pani.¹ Ba_5Ga_6 crystallizes in space group $P\bar{6}c2$ (No. 188). The beautiful structure shows isolated octahedral Ga_6 clusters sitting inside 12 Ba cuboctahedra.

This compound is interesting, because, as Fornasini and Pani noted in their paper, there is an unusual electron count for the Ga_6 cluster in this structure. If one assigns a +2 oxidation state to Ba, one obtains formally Ga_6^{10-} , which is two more electrons than required by the well-established polyhedral electron counting rules of Wade and Mingos.² We were intrigued by this problem and undertook a theoretical exploration of what distortions might have been expected in Ba_5Ga_6 and the possible reasons for their nonoccurrence.

Let us begin first with the well-known octahedral ion $\text{B}_6\text{H}_6^{2-}$. The extended Hückel (EH) molecular orbital (MO) method³ is used here to give us the energy level diagram of Figure 1. The parameters are specified in the Appendix. $\text{B}_6\text{H}_6^{2-}$ is here constructed from a boron octahedron and six terminal H's. As can be seen, 13 MO's are filled completely with 26 electrons, exactly the number of valence electrons available for $\text{B}_6\text{H}_6^{2-}$. There is a big gap of ~ 6 eV between the highest occupied molecular orbital (HOMO) (t_{2g} , one component out of three shown in 1) and the lowest unoccupied molecular orbital (LUMO) (t_{2u} ,

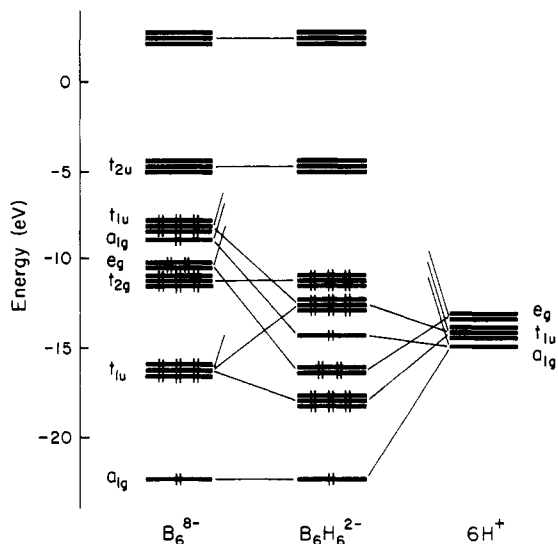
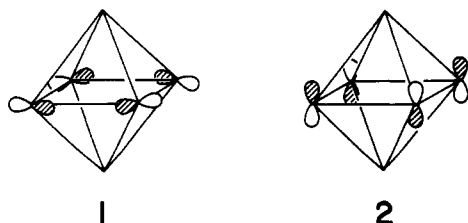


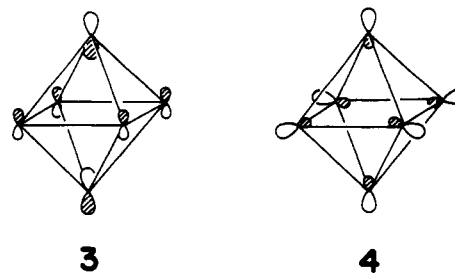
Figure 1. The levels of $\text{B}_6\text{H}_6^{2-}$ (center), constructed from a B_6^{8-} octahedron (left) and six protons (right).

closed-shell configuration for 13 occupied MO's. Now the t_{1u} , 3, is the HOMO and t_{2u} , 2 (the same one as for $\text{B}_6\text{H}_6^{2-}$), the LUMO.



one component out of three shown in 2), which is an indicator of stability for the compound. A qualitative bonding picture may be found also in refs 2, 4, 5, and 6.

Now imagine that six protons are pulled away from $\text{B}_6\text{H}_6^{2-}$. What is left behind is a B_6^{8-} cluster. Figure 1 at left actually shows the energy level diagram for that molecule. Though the HOMO–LUMO gap is smaller than for $\text{B}_6\text{H}_6^{2-}$, there is still a



Gallium and boron are in the same group in the periodic table. Thus, by analogy, a stable Ga_6^{8-} octahedron is expected. We carried out calculations on this cluster, the Ga–Ga bond length taken as 2.7 Å (close to the average of the values observed in Ba_5Ga_6) in a regular octahedron. In Figure 2 (left), we show the

[†] Dedicated to our friend C. N. R. Rao.

* Abstract published in *Advance ACS Abstracts*, August 15, 1994.

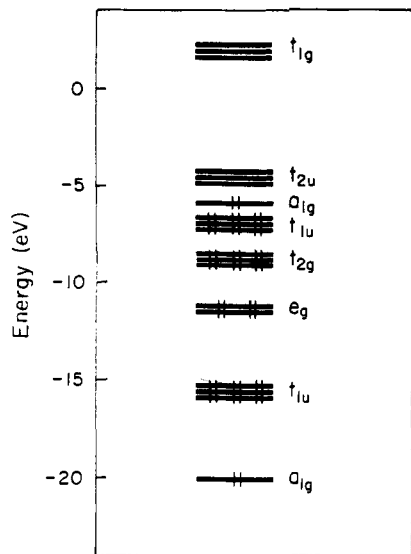


Figure 2. Energy level diagrams for a Ga₆⁸⁻ perfect octahedron with a 2.70 Å Ga–Ga near-neighbor distance.

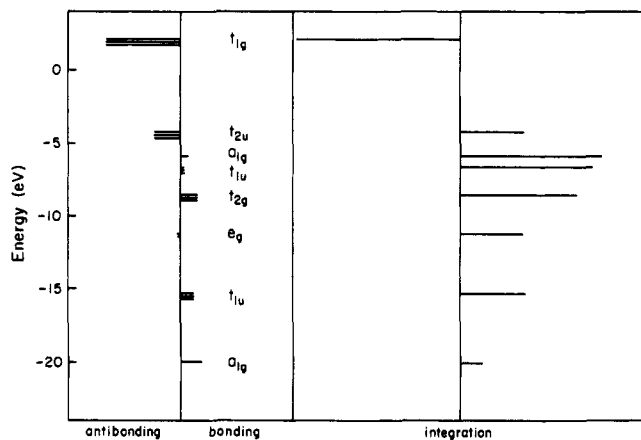


Figure 3. Molecular orbital overlap population plot of near-neighbor Ga–Ga bonds in the Ga₆ octahedron (left). At right is the integrated overlap population up to the energy level indicated.

orbitals of Ga₆. They are quite similar (as they should be) to those of an octahedral T_{1g} system reported recently.⁷ We can see that with 26 electrons, MO's through the HOMO a_{1g}, 4, are filled; the t_{2u} is again the LUMO. Using a Mulliken population analysis,⁸ we can easily identify bonding contributions from individual atomic orbitals (AO), atoms, fragment MO's (FMO), and MO's. The result is shown in Figure 3. Here we plot the overlap population of each level—to the right of the vertical line is bonding, to the left antibonding. All the occupied MO's are bonding in character, except the e_g which is a little bit antibonding. The magic number of 26 valence electrons provides maximum bonding.

However, two points are to be noted. First, filling LUMO t_{2u} would destabilize the Ga₆ octahedron, since t_{2u} is Ga–Ga antibonding. Second, a Ga₆ octahedron with 24 (or even 18) electrons is, in principle, possible, because the HOMO a_{1g} (and the t_{1u} right below it) is only slightly bonding. Such polyhedral clusters (Ga₆⁶⁻ and Ga₆, respectively) would have a closed-shell structure and their bonding should not be much weaker than that of Ga₆⁸⁻.

We now turn to Ba₅Ga₆. The first thing we did was to calculate an isolated molecular Ga₆ cluster cut out of the solid. In the Fornasini and Pani structure, such a Ga₆ cluster has six Ga–Ga distances of 2.70 Å, three of 2.71 Å, and three of 2.75 Å. The resulting levels are nearly indistinguishable from those of O_h Ga₆

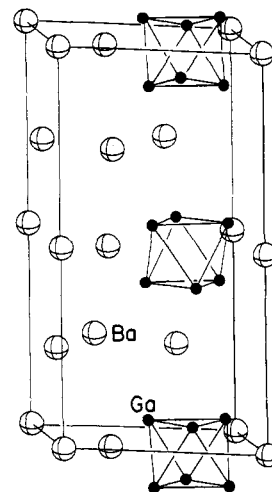


Figure 4. Unit cell of the Ba₅Ga₆ phase used in the extended Hückel calculations. Large spheres are Ba's and small (black) ones Ga's.

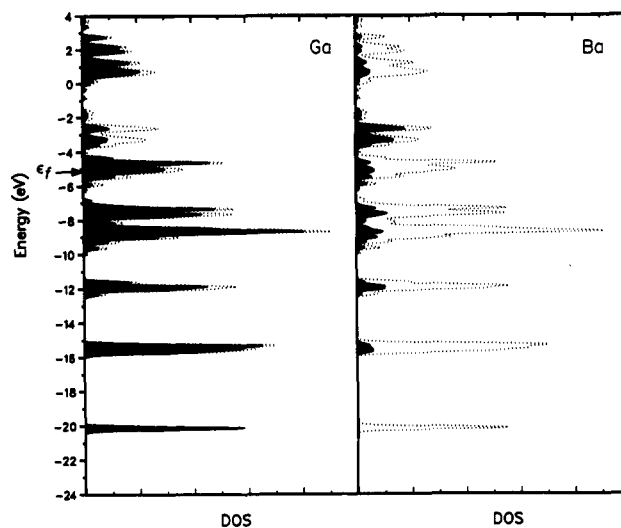


Figure 5. Density of states plots for the Ba₅Ga₆ phase. Dotted curves: the total DOS. The shaded areas: Ga contribution to the DOS (left), and Ba contribution to the DOS (right).

and we do not show them. There is a tiny splitting of the t_{2u}.

We next go on to the complete three-dimensional solid, using a slightly corrected description of the structure (space group P3c1, No. 158) with no disorder.⁹ The unit cell content for the extended solid is shown in Figure 4.

The results are plotted as a density of states (DOS),¹⁰ corresponding to an energy level diagram for molecules. In Figure 5 (left) are shown the total DOS (dotted curve) and the gallium contribution to that DOS (shaded area) of the Ba₅Ga₆ phase. The Ga atom contribution dominates below the Fermi level. Although the Ga DOS has a pattern similar to that of the molecular Ga₆ cluster (see Figure 2), differences are evident. There is some small mixing of Ba states below the Fermi level, as shown by the Ba contribution in Figure 5 (right), and their matching with Ga energies suggests these interactions are covalent in character. The total population of Ba states at the Fermi level is about 0.83 electrons per Ba, i.e., a net positive charge of 1.17.

The band shifts observed (relative to isolated cluster levels) could be caused by Ba–Ga interactions or by interactions between Ga₆ clusters. To distinguish between them, we did a calculation for the Ga-only substructure of Ba₅Ga₆ (12 Ga atoms in the unit cell). The results are shown in Figure 6. The contributions projected (shaded area) are for the a_{1g}- and t_{2u}-like MO's, respectively. Comparison with the isolated molecular Ga₆ cluster

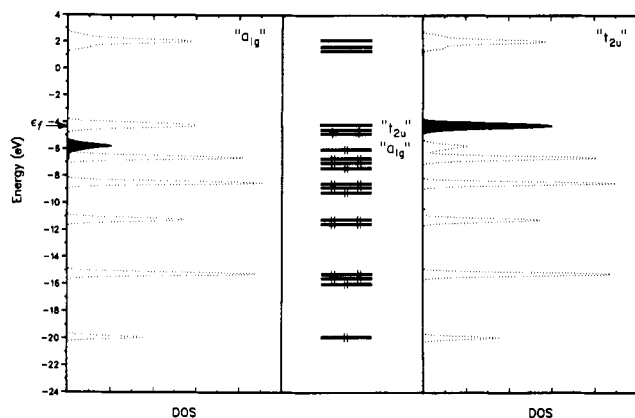


Figure 6. Density of states plots for the Ga-only substructure of the Ba_5Ga_6 phase. The total DOS is shown by dotted curves, the contribution of the a_{1g} -like FMO by the shaded area (left) and that of the t_{2u} -like FMO's by the shaded area (right). In the middle is the energy level diagram of the molecular Ga_6 cluster in Ba_5Ga_6 .

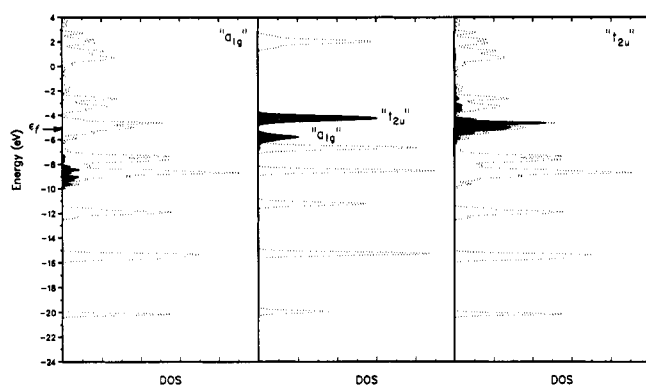


Figure 7. Density of states plots for the Ba_5Ga_6 phase with the total DOS (dotted curves), the contribution of the a_{1g} -like FMO (left, the shaded area) and that of the t_{2u} -like FMO's (right, the shaded area). In the middle is the DOS plot for the Ga-only substructure of the Ba_5Ga_6 phase, with the same FMO's projected.

levels (middle panel) reveals almost no difference. Thus, we conclude that in Ba_5Ga_6 the interaction between neighboring Ga_6 clusters is negligible.

Figure 7 shows the projected DOS's (shaded area) of a_{1g} - and t_{2u} -like FMO's in Ba_5Ga_6 . Both are broadened and pushed down in energy (significantly for the a_{1g}), compared with those of the Ga-only substructure. The latter were shown in Figure 6, and are repeated, for ease of making the comparison, in the middle of Figure 7. The significant perturbation of the a_{1g} - and t_{2u} -like FMO's is the result of Ba–Ga interactions in the crystal. The t_{1u} - and t_{2g} -like FMO's (not projected) right below the HOMO a_{1g} of Ga_6^{8-} are also pushed down. Those shifts of energy levels (all are bonding FMO's) are responsible for the electronic contribution to the stability of the Ba_5Ga_6 phase (total energy for 56 electrons per unit cell: -614.75 eV), compared with the Ga-only substructure (total energy for 56 electrons per unit cell with 12 Ga atoms: -577.09 eV). Our calculations do not explicitly include a presumably substantial Madelung energy component.

The Mulliken population analysis can be applied to extended structures as well as molecules, and the resulting crystal orbital overlap population (COOP)¹¹ is plotted in Figure 8 for the Ba–Ga and Ga–Ga bonds. The integrated average overlap population, up to the Fermi level, is 0.198 for Ba–Ga and 0.471 for Ga–Ga (compare the latter with 0.509 for isolated Ga_6^{8-} and 0.419 for Ga_6^{10-}). Up to the Fermi level, interactions between Ga atoms within the Ga_6 cluster are mostly bonding, and the Ba–Ga interactions are also mostly bonding! Interestingly, right below

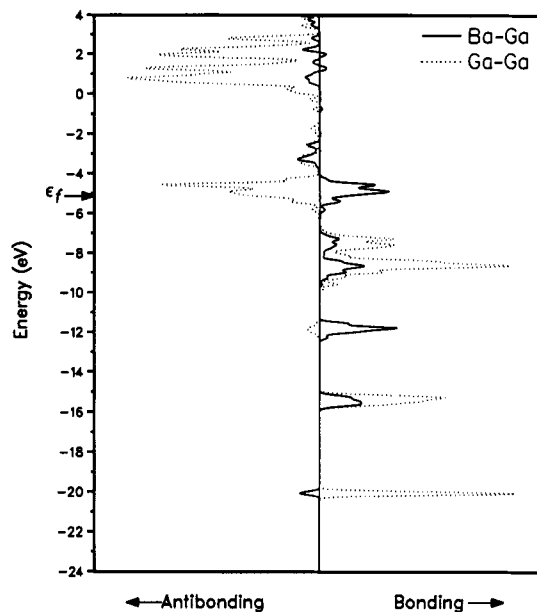


Figure 8. Crystal orbital overlap population plots for an averaged Ba–Ga bond (solid curve) and Ga–Ga bond (dotted curve) in the Ba_5Ga_6 phase.

the Fermi level, the Ba–Ga interaction is bonding, which diminishes somewhat the antibonding, destabilizing effect of filling the t_{2u} -like FMO. If this phase were oxidized a little, Ba–Ga bonding would weaken and Ga–Ga strengthen.

Our calculations also show that the interactions between Ba atoms are negligible, which is no surprise, since the separations are large (minimum Ba–Ba separation is 4.14 Å).

According to these calculations, a pure Ba_5Ga_6 phase would be a metallic conductor, since the Fermi level falls within an energy band, in a region of a substantial DOS (see Figure 5).

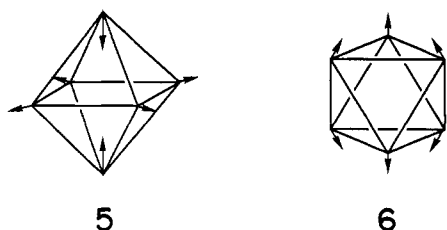
We return to the question of violation of the useful Wade–Mingos rules and the nature of the distortion one might have expected. The Fermi level in Ba_5Ga_6 lies in a band largely derived from the t_{2u} LUMO of an isolated Ga cluster. Thus we would have the solid-state analog of Ga_6^{10-} in this material. Note that this does not imply that the calculated (or real) charge distribution in Ba_5Ga_6 is $(\text{Ba}^{2+})_5\text{Ga}_6^{10-}$. The actual charges we compute are about 1.17⁺ on each Ba, and 5.85⁻ on each Ga_6 cluster. Nevertheless t_{2u} -like, slightly Ga–Ga antibonding, levels are partially occupied.

Supposing one had Ga_6^{10-} as an isolated cluster, what geometrical distortion might one expect in it? One line of reasoning (Wade–Mingos) is that an electron count in excess of the magic number will induce one (or more) bond to cleave, moving from a *closo* to a *nido* cluster. A second line of reasoning (Jahn–Teller-like) would argue as follows: We have a $(t_{2u})^2$ configuration. What symmetry-lowering vibration will split t_{2u} so that one level goes below two, stabilizing a low-spin configuration? Many vibrations can do this, but the higher subgroups of O_h in which this is achieved are D_{4h} or D_{3d} .

It may be noted that for a Jahn–Teller argument to work, i.e., for a symmetry-allowed distortion actually to occur, one has to have “the orbital power” to do so. What is meant by this is that the relevant orbitals, split by a perturbation, must be substantially bonding or antibonding in the region of the deformation. Otherwise the levels will split, but minutely so, and no static deformation will be observed. Note from Figure 3 or 8 that the t_{2u} orbital is somewhat Ga–Ga antibonding.

We have calculated deformations of a Ga_6^{10-} octahedron which reduce the symmetry to D_{4h} or D_{3d} , corresponding to normal

modes 5, e_g and 6, t_{2g}, respectively. This was done first for an isolated molecular cluster.



We obtained the expected double-well curves, with the O_h geometry being a maximum with respect to both D_{4h} and D_{3d} distortions. We went on to the full extended Ba₅Ga₆ structure. This was done by substituting the C₃ Ga₆ clusters in Ba₅Ga₆ with O_h and D_{3d} clusters. The computed potential energy surface for distortions lowering the local Ga₆ symmetry from O_h led essentially to the same result as for Ga₆¹⁰⁻; i.e., distortion was favored, contrary to the observed structure. We do note that the closed-shell Ga₆⁸⁻ cluster is stable with respect to the same deformations in the isolated cluster.

Actually, we had better be careful in our predictions for the clusters that do have closed-shell electron counts, for nature has a way of coming up with surprises. Recently, the structures of KTI and CsTI were determined. These contain octahedral clusters and are formally Tl₆⁶⁻, i.e., with four fewer electrons than our Ga₆¹⁰⁻. The level ordering for O_h Tl₆⁶⁻ is exactly as we have for Ga₆⁶⁻ in Figure 2. If the a_{1g} were empty, one would have a closed shell, and no distortion would be predicted. In fact the octahedra are strongly tetragonally compressed (to D_{2h} or D_{4h} site symmetry, respectively).⁷

Computations on the isolated cluster show a strong splitting of the t_{1u} level for such a distortion, one component of it rising above the a_{1g}, and producing a closed shell D_{4h} distorted system. So here is a case of a system that one might have thought should not distort in fact does so. The matter is somewhat complicated because the extended structure environment could affect the a_{1g}-t_{1u} level order. It does so in Ba₅Ga₆.

Given that we predict symmetry-lowering deformations for isolated Ga₆¹⁰⁻ clusters, and even for the solid (not that we trust the extended Hückel energetics so much), why is the deformation in the Ba₅Ga₆ phase so small? An unexpected, tentative, but satisfying answer comes, quite as a surprise, from work on some related phases. There is good, but indirect, evidence that the Ba₅Ga₆ phase might be Ba₅Ga₆H₂ instead.⁹ Normal Ba sources contain quite a lot of hydrogen, and this can determine phase stability in related case, e.g., Sr₅Sb₃H.¹² Formally, Ba₅Ga₆H₂ would have Ga₆⁸⁻ clusters in it, if hydrogen were counted as H⁻. The Wade-Mingos rules would then be satisfied; the Ga₆⁸⁻ cluster would not be expected to undergo Jahn-Teller distortions.

H⁻ is quite big (crystal radius 1.10–1.22 Å^{13,14}). Is there any space for hydrides in the Ba₅Ga₆ structure? Using a program written by one of us (QL), we located several sufficiently big holes in the Ba₅Ga₆ structure. These are shown in Figure 9. Within the unit cell, two holes lie between the Ga₆ clusters (type I, 2c position in this space group, surrounded by 6 Ga's at 2.92 Å and 3 Ba's at 2.77 Å), and two holes are in a line along the c-direction, going through distorted Ba tetrahedra (sharing one face and one vertex alternatively) (type II, 2b position, 4 Ba's at 2.70 Å). Two distorted tetrahedral Ba holes are also found along the c-edge (type III, 2a position, 4 Ba's at 2.74 Å). 10 slightly smaller cavities (four surrounded by 4 Ba atoms, and six by 2 Ga's and 3 Ba's at about 2.60 Å) are also present in the structure.

Putting H⁻ into these holes, we found the minimum total energy for Ba₅Ga₆H₂ with two H⁻'s in type II holes and two H⁻'s in type III ones per unit cell ($Z = 2$). Our computations show a net negative charge of 0.78 on each H. The 4 H⁻'s inserted exert a

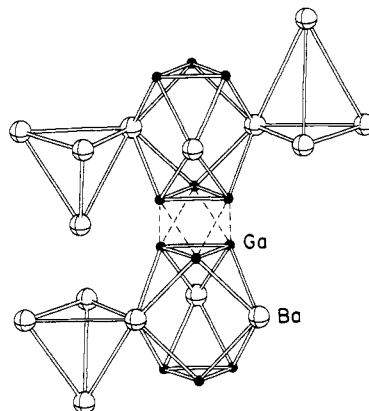


Figure 9. Holes in the Ba₅Ga₆ structure. Two type I holes are shown between clusters in the middle, two type II are on the left, and one type III is on the right. Large spheres are Ba's and small (black) ones Ga's.

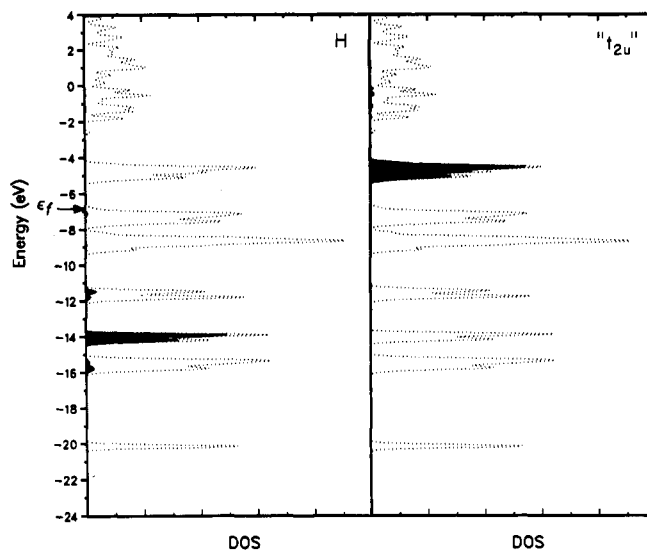


Figure 10. Density of states of Ba₅Ga₆H₂. Two H's are in type II holes and two H's in type III ones. The shaded area is the contribution of all H's (left) and that of t_{2u}-like FMO's (right).

relatively small electronic perturbation on Ba₅Ga₆, which is supported by the H atom DOS projection (Figure 10, left), a single sharp peak around -14 eV.

Some significant changes are observed in the DOS plot of Ba₅Ga₆H₂ (Figure 10). The Fermi level is lowered from -5.12 (Ba₅Ga₆) to -6.80 eV, the t_{2u}-like orbitals (Figure 10, right) are not occupied (and become less disperse), and a gap of ~0.6 eV opens up between the valence band and the conduction band. Thus the Ba₅Ga₆H₂ phase should be a semiconductor. For hydrogen-free Ba₅Ga₆, we would expect, as we said earlier, a metallic material. The published work does not indicate the conductivity of the material.

We also tried putting more H into the structure, since there is room for it. Our calculations show that Ba₅Ga₆H₃ and Ba₅Ga₆H₄ are favored energetically over Ba₅Ga₆. But such phases would have distorted octahedral Ga₆ clusters in them, since both have partially filled bands and are susceptible to Jahn-Teller effect. Also, BaH₂ + BaGa₂ is an obvious alternative to the Ba₅Ga₆H₄ compound.

Let us summarize our main conclusions here:

1. The Wade-Mingos rules predict maximum bonding interactions for a Ga₆ cluster with 26 electrons (Ga₆⁸⁻), but 18- and 24-electron counts are also possible, in isolation and in solid-state compounds. A Ba₅Ga₆ phase would indeed constitute an example of violation of the Wade-Mingos rules in an extended structure.

TABLE 1: EH Parameters

atom	orbital	H_{ii} (eV)	ζ_{ii}
H	1s	-13.60	1.30
B	2s	-15.20	1.30
	2p	-8.50	1.30
Ga	4s	-14.58	1.77
	4p	-6.75	1.55
Ba	6s	-6.32	1.23
	6p	-3.85	1.23

2. Both Ga–Ga interactions within the Ga_6 cluster and Ba–Ga interactions are bonding, stabilizing a hypothetical Ba_5Ga_6 phase.

3. A Jahn–Teller type distortion would be expected for the Ga_6 cluster in Ba_5Ga_6 , of a magnitude greater than that observed.

4. We think it is likely, however, that the Ba_5Ga_6 phase is $Ba_5Ga_6H_2$. The H⁻s should enter tetrahedral holes formed by Ba's. And $Ba_5Ga_6H_2$ should be semiconducting.

5. The following suggestions may be made for future synthetic exploration: Reasonable electron counts could be obtained for (a) isolated 26-electron Ga_6 clusters, e.g., $M_2X_3Ga_6$ ($M = K, Rb,$ or $Cs, X = Ba, Sr,$ or Ra); (b) isolated 24-electron Ga_6 clusters, e.g. M_4XGa_6 ($M = K, Rb,$ or $Cs, X = Ba, Sr,$ or Ra).

Acknowledgment. Q.L. thanks Haibin Deng and Kimberly Lawler for help in using the extended Hückel program, William Shirley for help in using computers, and the Hoffmann research group for useful discussion. We are grateful to the National Science Foundation for supporting this work through Research

Grant CHE8912070, and to the Materials Science Division, Department of Energy, for support through Contract No. W-7405-Eng-82.

Appendix

Table 1 shows the extended Hückel method parameters used in our calculations. For H, B, and Ga, values are taken from earlier work.^{3,15,16}

In computing the solid structure, a 18 k-point set for the hexagonal unit cell was used to calculate averaged properties.

References and Notes

- (1) Fornasini, M. L.; Pani, M. *J. Alloys Compd.* **1994**, *205*, 179.
- (2) Albright, T. A.; Burdett, J. K.; Whangbo, M.-H. *Orbital Interactions in Chemistry*; Wiley-Interscience: New York, 1985; Chapter 22.
- (3) Hoffmann, R. *J. Chem. Phys.* **1963**, *39*, 1397.
- (4) Greenwood, N. N.; Earnshaw, A. *Chemistry of the Elements*; Pergamon: Oxford, 1984; p 182.
- (5) Wade, K. *J. Chem. Soc., Chem. Commun.* **1971**, 792.
- (6) Mingos, D. M. P.; Wales, D. J. *Introduction to Cluster Chemistry*; Prentice-Hall: Englewood Cliffs, NJ, 1990.
- (7) Dong, Z.; Corbett, J. D. *J. Am. Chem. Soc.* **1993**, *115*, 11299.
- (8) Hoffmann, R. *Solids and Surfaces: a Chemist's View of Bonding in Extended Structures*; VCH: New York, 1988; p 32.
- (9) Zhao, J.-T.; Leon-Escamilla, E. A.; Corbett, J. D., unpublished research.
- (10) Reference 8, page 26.
- (11) Reference 8, page 43.
- (12) Leon-Escamilla, E. A.; Corbett, J. D. *J. Alloys Compd.* **1994**, *206*, L15.
- (13) Corbett, J. D.; Marek, H. S. *Inorg. Chem.* **1983**, *22*, 3194.
- (14) Shannon, R. D. *Acta Crystallogr.* **1976**, *A32*, 751.
- (15) Anderson, A. B.; Hoffmann, R. *J. Chem. Phys.* **1974**, *60*, 4271.
- (16) Canadell, E.; Eisenstein, O.; Rubio, J. *Organometallics* **1984**, *3*, 759.